



# How to transform the standing man from a box to a cylinder – a modified methodology to calculate mean radiant temperature in field studies and models

Björn Holmer<sup>1</sup>, Fredrik Lindberg<sup>1</sup>, David Rayner<sup>1</sup>, Sofia Thorsson<sup>1</sup>

<sup>1</sup> Dept of Earth Sciences, University of Gothenburg, Box 430, S-405 30 Gothenburg, Sweden  
Corresponding author: [bjorn@gvc.gu.se](mailto:bjorn@gvc.gu.se)

28 May 2015

## 1. Introduction

Mean radiant temperature ( $T_{mrt}$ ) has shown to be an important meteorological variable in studies of human comfort and health. The  $T_{mrt}$  is defined as the ‘uniform temperature of an imaginary enclosure in which the radiant heat transfer from the human body equals the radiant heat transfer in the actual non-uniform enclosure’ (ASHRAE, 2001). One way to obtain  $T_{mrt}$  is to calculate the surface temperature of a standing man approximated as a cylinder emitting the same amount of longwave radiation as all short- and longwave radiation fluxes received from the surrounding four cardinal points and down- and upwards. Fig. 1 shows an example of the equipment that can be used. The calculation was introduced by Höppe in (1992) and has then been used both in models (e.g. SOLWEIG) (Lindberg, Holmer, & Thorsson, 2008) and field studies (Kantor, Kovacs, & Lin, 2014; Kantor, Lin, & Matzarakis, 2014; Thorsson, Lindberg, Eliasson, & Holmer, 2007). However, the formula by Höppe describes in fact a man shaped like a box and not a cylinder as noted by Kantor, Lin, et al. (2014). The box shape has resulted in some peculiar features noticed in studies of  $T_{mrt}$  such as a local minimum at noon (e.g. Kantor, Kovacs, et al. (2014); Kantor, Lin, et al. (2014); Mayer, Holst, and Imbery (2009); Thorsson et al. (2007)) and an influence of the orientation of the field equipment (Kantor, Lin, et al., 2014). These anomalies occur not only in  $T_{mrt}$  calculated from field data but also in model calculations based on the Höppe formula, e.g. SOLWEIG. Thus the anomalies are caused by the calculation method and not connected to shortcomings of the equipment.

We propose a new method for calculating  $T_{mrt}$  for a cylinder that overcomes the anomalies generated by the original calculation by Höppe. Fig. 2 shows to the left the  $T_{mrt}$  on a sunny day in Ouagadougou, Burkina Faso calculated with the initial formula by Höppe and also with the new methodology. As shown the midday secondary minimum has disappeared and is replaced with a maximum. On the other hand the broad “shoulders” of the initial calculation have been diminished. The maximum now occurs when the solar elevation is highest and there is a slight asymmetry to the hours after noon depending on a higher proportion of longwave radiation due to higher surface and air temperatures of the surroundings. To the right in fig. 2 the  $T_{mrt}$  on a sunny autumn day in Gothenburg, Sweden is shown. The equipment was oriented along the buildings instead of in north-south direction and due to this deviation (9°) the calculation according to the old method became very asymmetrical. However, with the new methodology this orientation was accounted for and maximum was obtained at 1 p.m. and as in Ouagadougou the distribution had a slight asymmetry.



Fig. 1. Equipment to monitor the short- and longwave fluxes in six directions

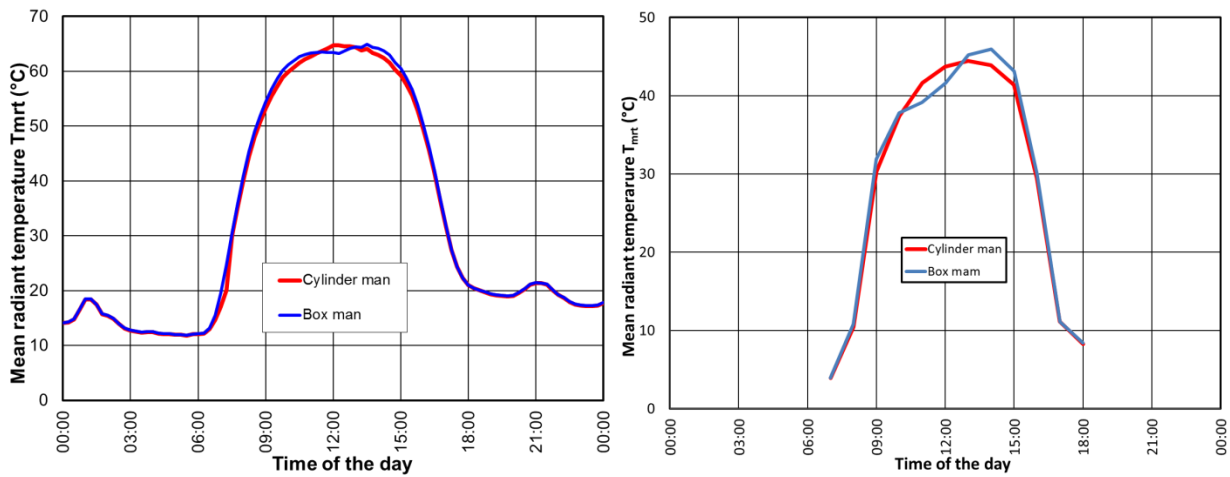


Fig. 2.  $T_{mrt}$  in based on six-directional monitoring of short- and longwave radiation. Calculation of  $T_{mrt}$  according to the original formula by Höppe (box man) and with the new methodology (cylinder man). Left: Ouagadougou, Burkina Faso on 10<sup>th</sup> of December 2007 and Right: Gothenburgh, Sweden on 11<sup>th</sup> of October, 2005

## 2. The new methodology

In the Höppe formula the short- and longwave fluxes in six directions each are used as input. They are multiplied with surface fractions ( $w_i$ ) of the standing man and adjusted according to the albedo ( $\alpha$ ) and emissivity ( $\epsilon$ ) factors. These absorbed amounts of radiation are summed up to the mean radiant flux  $S_{str,box}$ :

$$S_{str,box} = \underbrace{(1-\alpha) \cdot \sum w_i \cdot K_i}_{\text{shortwave}} + \underbrace{\epsilon \cdot \sum w_i \cdot L_i}_{\text{longwave}} \quad \dots(1)$$

Thus  $S_{str,box}$  comprises of a shortwave and a longwave component derived in a similar way based on the six directions. The  $T_{mrt}$  is then calculated as:

$$T_{mrt} = (S_{str,box} / (\epsilon\sigma))^{0.25} - 273.15 \quad \dots(2)$$

where  $\sigma$  is Stefan-Boltzmann's constant.

There are two issues that had to be handled in the new methodology. The first is that the shortwave radiation has two parts – direct and diffuse. The diffuse radiation comes from all points of the sky and is presumed to be isotropic while the direct only comes from one point, i.e. the Sun. This means that the diffuse radiation can be absorbed on the whole surface of the standing man. The second issue is that the direct radiation is only absorbed by the surface of the standing man (perpendicular to the direct radiation) that is exposed to the sun. The size of this surface varies with the latitude, the time of the year and the time of the day, while the absorbing surface to diffuse radiation always is the same. Also the longwave radiation is received from the whole surrounding and there will be no changes of the absorbing surface. The new methodology requires data on solar elevation and azimuth for every time step.

Despite that the observed shortwave radiation fluxes include both direct and diffuse radiation it is possible to divide them into the two components since there always will be two of the sensors that are not sunlit (or one if the direct radiation has the same direction as the sensor axis). Thus the minimum value of the four sensors monitoring the horizontal shortwave fluxes is presumed to give the diffuse radiation<sup>1</sup>:

$$K_{diff} = \min(K_E, K_S, K_W, K_N) \quad \dots(3)$$

Then the direct component ( $S_{dir,i}$ ) is obtained by subtraction of the diffuse component:

$$K_{dir,i} = K_{obs,i} - K_{diff} \quad \dots(4)$$

There are usually two sensors that are receiving direct radiation. The resultant horizontal direct radiation ( $K_{dir,hor}$ ) flux is obtained by the Pythagorean Theorem:

<sup>1</sup> This “diffuse” radiation can include some reflected radiation. Maybe it should be better to use the term “base” radiation.

$$K_{dir,hor} = \sqrt{(K_{dir,left}^2 + K_{dir,right}^2)} \quad \dots(5)$$

where “left” and “right” denote the  $K_{dir,i}$  at both sides of the adjusted (see below) azimuth of the direct radiation.

Finally, the direct radiation along the sun rays is:

$$K_{dir} = K_{dir,hor} \cdot \cos(\beta) \quad \dots(6)$$

where  $\beta$  is the solar elevation above the horizon.

However, often there is also reflected radiation ( $K_{ref}$ ). This is obtained from the two sensor that frames the opposite quadrant in the same way as  $K_{dir,hor}$  and the total direct radiation flux is then:

$$K_{dir,tot} = K_{dir,hor} \cdot \cos(\beta) + K_{ref,hor} \cdot \cos(\beta) = (K_{dir,hor} + K_{ref,hor}) \cdot \cos(\beta) \quad \dots(7)$$

assuming the reflecting surfaces are vertical and act like mirrors so the angle of the reflected radiation is  $\beta$ .

The orientation of the equipment at the installation is probably guided by a compass. However, the magnetic field does not point to the true geodetic north and further an urban environment contains electromagnetic fields that disturb the compass orientation. Therefore the orientation of the equipment had to be checked and adjusted so that the adjusted azimuth is zero when the direct radiation has the same direction as the sensor axis. This adjustment is important to be able to choose the quadrant for the calculation of resultant horizontal direct radiation ( $K_{dir,hor}$ ) with the Pythagorean Theorem. The adjustment is done via the “observed” direct radiation during a clear sky situation. This is easily tested by plotting the direct radiation for the east and west looking sensors in relation to the astronomical azimuth around noon. The azimuth angle at the intersect of the two curves gives the correction, i.e. with minimum direct radiation on the east and west looking sensors. Fig. 3 shows an example.

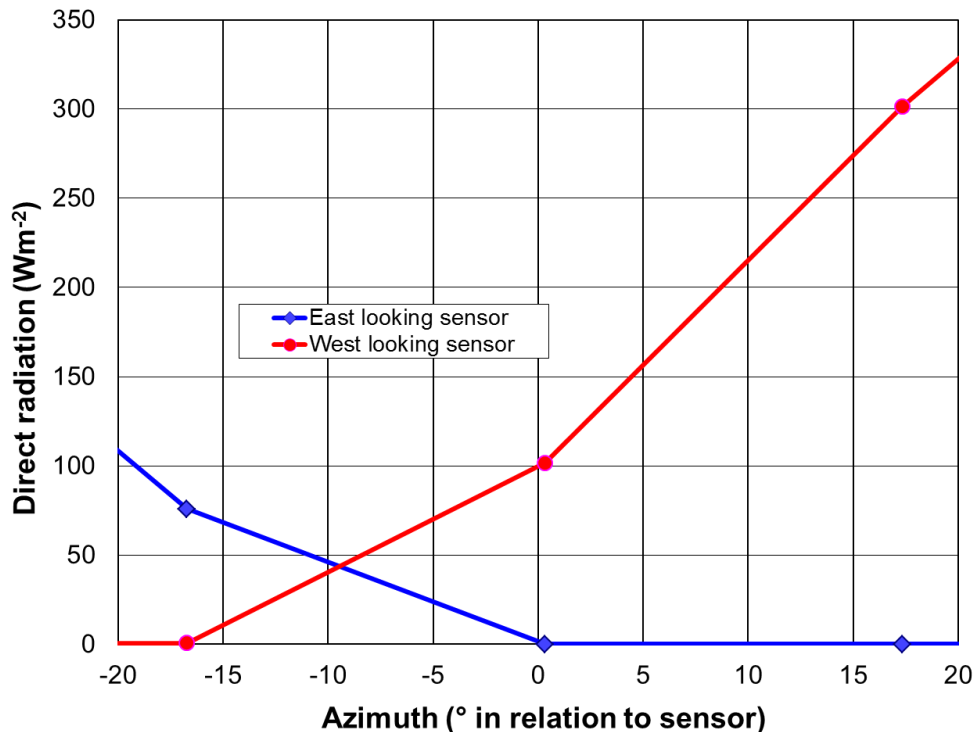


Fig. 3. Plot of direct shortwave radiation fluxes from east ( $K_E$ ) and west ( $K_W$ ). The intersect shows that the sensor azimuth needs to be corrected with about 9°.

The fractions in different directions of the surfaces of the standing box man are often assumed to be: up and down 0.06 each and 0.88 ( $4 \times 0.22$ ) for the vertical exposure. The same fractions are assumed for the new standing cylindrical man.

The vertical area of the cylinder is 0.88 of the total cylinder area but the maximum area exposed to the sun (at sunrise and sunset, i.e.  $\beta = 0$ ) is 0.28, since the cylinder surface is  $\pi$  times higher than a rectangle with the same proportions as the cylinder.

The surface (perpendicular to the radiation) exposed to the sun ( $A_{dir}$ ) is then:

$$A_{dir,cyl} = 0.28 \cdot \cos(\beta) + 0.06 \cdot \sin(\beta) \quad \dots(8)$$

including the sunlit area of the top of the cylinder.

This can be compared with the standing box man:

$$A_{dir,box} = 0.22 \cdot [\cos(\gamma) + \sin(\gamma)] \cdot \cos(\beta) + 0.06 \cdot \sin(\beta) \quad \dots(9)$$

where the exposed surface also is influenced by the angle ( $\gamma$ ) of the difference between the azimuth of the sun and the direction of the equipment axis. The value of  $(\cos(\gamma) + \sin(\gamma))$  varies between 1 and 1.41. Fig. 4 shows how the sunlit ratio of the whole “body” varies with solar height. All “bodies” have the same area exposed to direct radiation when the sun is at zenith. But at lower sun angles the sun exposed fraction depends on the shape of the standing man and for the box man also the solar azimuth. For example, with an N-S orientation of the equipment the exposed surface is 1.41 times larger at 9 a.m. or 3 p.m. than at noon.

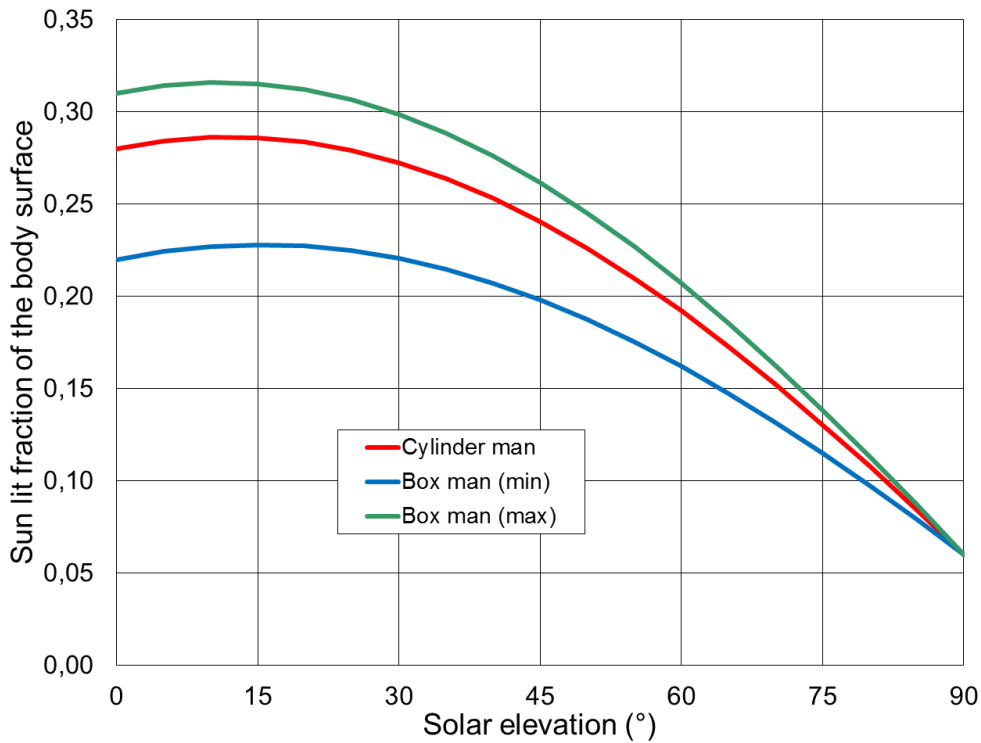


Fig. 4. Sun exposed fraction of the standing man perpendicular to the direct radiation in relation to the solar angle above the horizon.

To sum up, the total amount of short- and longwave radiation absorbed by the cylindrical man ( $S_{str,cyl}$ ) is:

$$S_{str,cyl} = (1-\alpha) \cdot \underbrace{[0.28 \cdot \cos(\beta) \cdot K_{dir,tot}]_{\text{horizontal direct}} + \underbrace{0.06 \cdot (K_{\uparrow} + K_{\downarrow})}_{\text{vertical global}} + \underbrace{0.22 \cdot \Sigma K_{\rightarrow j}}_{\text{horizontal diffuse}} + \underbrace{\epsilon \cdot \Sigma w_i \cdot L_i}_{\text{longwave}} \quad \dots(10)$$

-----  
shortwave

where 
$$K_{dir,tot} = \cos(\beta) \cdot \sqrt{(K_{dir,left}^2 + K_{dir,right}^2)} \quad \dots(11)$$

### 3. Implementation in models - the SOLWEIG model

Direct shortwave radiation is together with global radiation input in the SOLWEIG model (Lindberg et al., 2008). Thus it is easy to rearrange the calculations to for the new methodology. It is also easy to change the standing man from a box to a cylinder.

A most interesting aspect of the model is that one output is a map of  $T_{mrt}$  and not only data for a single point. In fig. 2 it can be seen that the maximum values of  $T_{mrt}$  do not differ much between the two methods. However, since the timing of the high values differs between the two calculations it can be of interest to analyze the distribution of  $T_{mrt}$ . Fig. 5 shows  $T_{mrt}$  maps based on the cylinder man in Gothenburg during an autumn day at 1 p.m. (left) when  $T_{mrt}$  is close to the maximum based on the cylinder man and at 3 p.m. (right) when  $T_{mrt}$  based on the box man has its maximum. There are also difference maps of the two methods to show the details of the position and magnitude of the differences.

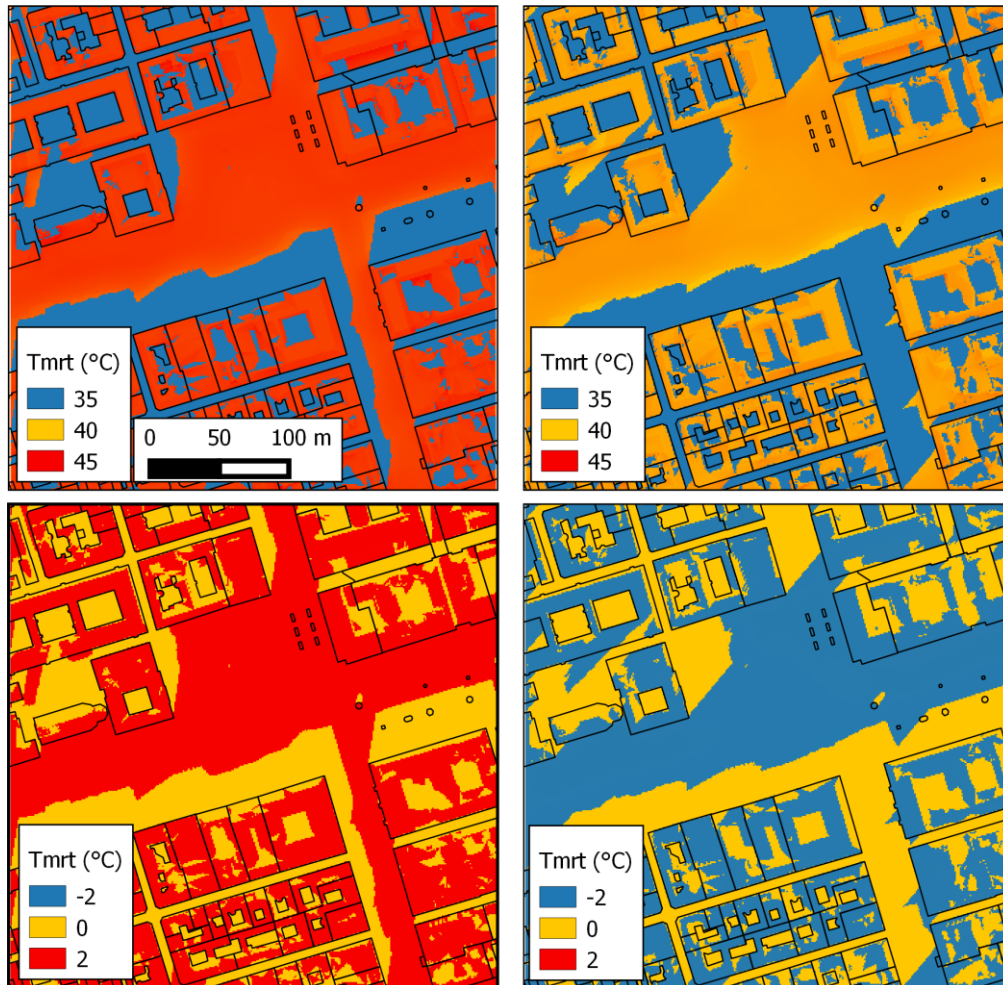


Fig. 5.  $T_{mrt}$  in Gothenburg on the 11<sup>th</sup> of October 2005 calculated with SOLWEIG. a/  $T_{mrt}$  at 1 p.m. according to the cylinder man, b/  $T_{mrt}$  at 3 p.m. according to the cylinder man, c/ differences at 1 p.m. in  $T_{mrt}$  between the box man and the cylinder man and d/ differences at 3 p.m. in  $T_{mrt}$  between the box man and the cylinder man.

The range of  $T_{mrt,cyl}$  is larger at 1 p.m. (Fig. 5a) than at 3 p.m. (Fig. 5b) and the distribution has no pixels around 40°C. Thus the differences in heat at different spots in the area are accentuated. Over the whole area the unshaded area  $T_{mrt,cyl}$  is higher than  $T_{mrt,box}$  (Fig. 5c). Compared with the situation at 3 p.m. when  $T_{mrt,box}$  had maximum there are smaller shadow areas at 1 p.m. and thus larger areas with enhanced heat. At 3 p.m. near maximum  $T_{mrt,box}$ ,  $T_{mrt,cyl}$  is lower all over the area (Fig. 5d).

#### 4. Concluding remarks

The data sets analyzed so far are from two different latitudes, 11°N and 58°N, and from two different climate zones. The new calculations show a maximum around noon and an acute distribution during clear skies. However, the influence of clouds is not analyzed in details but when looking at the formulas,  $T_{mrt}$  when it is overcast will most probably differ little from the previous calculations since the direct radiation vanishes. Another aspect that is not tested is the performance in environments with much reflected radiation but the differences between the two methods will probably become smaller than for open sites.

A major advantage of the new methodology is that the ambiguities that can be raised around the errors of the hitherto calculations can be put aside and the reliability of the interpretations will increase.

## 5. Addendum

Sometimes a globe thermometer is used to obtain  $T_{mrt}$ . To compare such measurements it can be useful to calculate a globe from the radiation fluxes instead of a standing man. The shortwave part of the radiation becomes simpler to calculate since the area of the direct radiation is the same all the time (0.25 of the globe surface area) irrespective of the solar angle:

$$S_{str,globe} = (1-\alpha) \cdot [0.25 \cdot K_{dir} + 1/6 \cdot \sum k_{diff,i}] + \varepsilon \cdot \sum W_i \cdot L_i \quad (13)$$

Fig 6a shows the  $T_{mrt}$  for a globe compared with a cylindrical standing man in Ouagadougou. In the middle of the day with a solar angle of 55° the sun exposed standing man surface is 0.21 while the sunlit globe surface is 0.25. Thus the globe gains more radiation and gets a higher  $T_{mrt}$ . During the night the  $T_{mrt}$  of the globe becomes slightly lower due to the larger area exposed upward (0.25 compared to 0.06) and a lesser downward longwave flux than in other directions as the emissivity of the sky is low. Contrary to Ouagadougou, in Gothenburg the globe  $T_{mrt}$  (Fig. 6b) is lower during most of the day as an effect of the low solar angle (30° at noon). As a result a larger amount of radiation is absorbed on the larger vertical sides of the standing man while the weaker vertical fluxes have greater importance in the globe calculation.

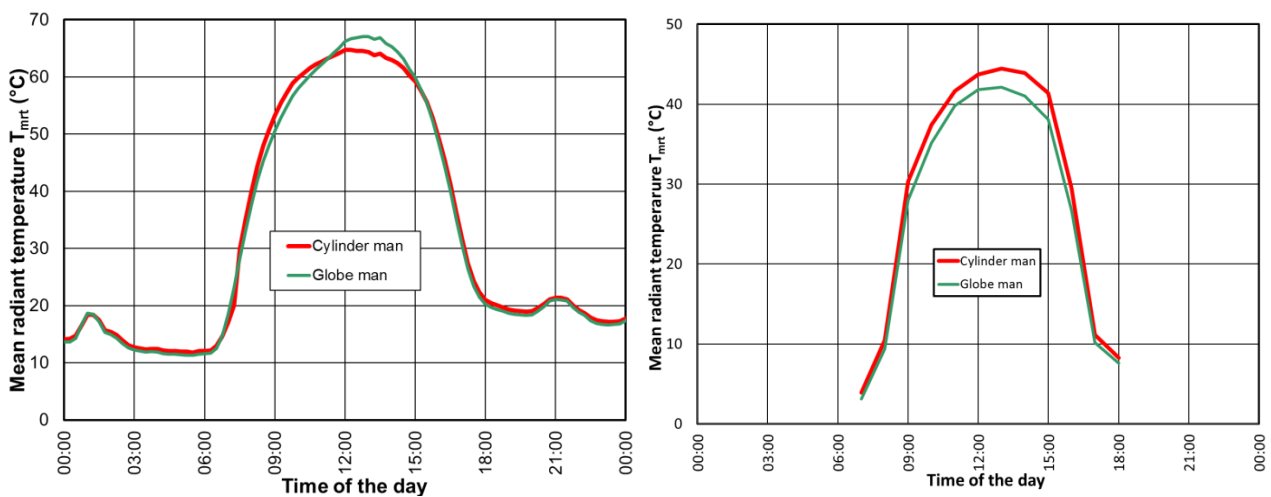


Fig. 6. Comparison  $T_{mrt}$  calculated with a cylindrical standing man and with a globe. a/  $T_{mrt}$  in Ouagadougou on the 10<sup>th</sup> of December 2007. Maximum solar elevation 55°. b/  $T_{mrt}$  in Gothenburg on the 11<sup>th</sup> of October 2005. Maximum solar elevation 30°.

## References

- ASHRAE. (2001). *ASHRAE fundamentals handbook 2001 (SI Edition)*: American Society of Heating, Refrigerating, and Air-Conditioning Engineers, USA.
- Höppe, P. (1992). Ein neues Verfahren zur Bestimmung der mittleren Strahlungstemperatur in Freien. *Wetter und Leben*, 44, 147-151.
- Kantor, N., Kovacs, A., & Lin, T.-P. (2014). Looking for simple correction functions between the mean radiant temperature from "standard black globe" and "six-directional" techniques in Taiwan. *Theoretical and Applied Climatology*.
- Kantor, N., Lin, T.-P., & Matzarakis, A. (2014). Daytime relapse of the mean radiant temperature based on the six-directional method under unobstructed solar radiation. *International Journal of Biometeorology*, 58, 1615-1625.
- Lindberg, F., Holmer, B., & Thorsson, S. (2008). SOLWEIG 1.0 - Modelling spatial variations of 3D radiant fluxes and mean radiant temperature in complex urban settings. *International Journal of Biometeorology*, 52, 697-713.
- Mayer, H., Holst, J., & Imbery, F. (2009). *Human thermal comfort within urban structures in a central European city*. Paper presented at the The seventh International Conference on Urban Climate, Yokohama.
- Thorsson, S., Lindberg, F., Eliasson, E., & Holmer, B. (2007). Different methods for estimating the mean radiant temperature in an outdoor urban setting. *international Journal of Climatology*, 27, 1983-1993.